Molecular Crystals and Liquid Crystals Incorporating Nonlinear Optics

Publication details, including instructions for authors and subscription information:
http://www.tandfonline.com/loi/gmcl17

Photoacoustic Thermal Characterisation of Liquid Crystals

J. Thoen [a], C. Glorieux [a], E. Schoubs [a] & W. Lauriks [a]

[a] Laboratorium voor Akoestiek en Warmtegeleiding, Departement Natuurkunde, Katholieke Universiteit Leuven, Celestijnenlaan 200 D, B-3030, Leuven, Belgium

Version of record first published: 22 Sep 2006.

To cite this article: J. Thoen , C. Glorieux , E. Schoubs & W. Lauriks (1990): Photoacoustic Thermal Characterisation of Liquid Crystals, Molecular Crystals and Liquid Crystals Incorporating Nonlinear Optics, 191:1, 29-36

To link to this article: http://dx.doi.org/10.1080/00268949008038576

Mol. Cryst. Liq. Cryst. 1990, Vol. 191, pp. 29–36
Reprints available directly from the publisher
Photocopying permitted by license only

Printed in the United States of America

Photoacoustic Thermal Characterisation of Liquid Crystals†

J. THOEN, C. GLORIEUX, E. SCHOUBS and W. LAURIKS

Laboratorium voor Akoestiek en Warmtegeleiding, Departement Natuurkunde, Katholieke Universiteit Leuven, Celestijnenlaan 200 D, B-3030 Leuven, Belgium

(*Received September 29, 1989*)

A completely automatic photoacoustic setup with microphone detection, allowing the simultaneous measurement of the heat capacity and the thermal conductivity of small liquid crystal samples, has been used to investigate heptylcyanobiphenyl (7CB) in the isotropic and in the nematic phase. Measurements have been carried out with and without a magnetic field and for different modulation frequencies.

Keywords: photoacoustic effect, heat capacity, thermal conductivity, anisotropy, phase transitions.

1. INTRODUCTION

The measurements of the thermal quantities of liquid crystals play an important role for locating the different phases and phase transitions. Although the technique of differential scanning calorimetry (DSC) is rather well established and of great practical importance, it is not very reliable for detailed studies of pretransitional behavior. It is e.g. also not very suitable for distinguishing between second order and weakly first order phase transitions.[1] High resolution calorimetric measurements, in particular near phase transitions, are usually carried with ac calorimetric techniques[2,3] or by adiabatic scanning calorimetry.[1,4] In both cases one obtains only information on static quantities: the heat capacity and the enthalpy. In a more complete thermal characterisation one would also like to get information on thermal transport properties such as the thermal conductivity and thermal diffusivity. The dynamic thermal behavior of liquid crystals has not been investigated in much detail. A number of thermal conductivity results has been obtained by means of conventional steady-state or transient methods.[5–7] These methods have the disadvantage of requiring large samples and sizable temperature gradients, making them e.g. unsuitable for detailed studies of phase transitions. Some high-resolution

†Part of the invited talk C2 presented at the 8th Liquid Crystal Conference of Socialist Countries, August 28–September 1, 1989, Krakow, Poland.

ac techniques, e.g. forced Rayleigh light scattering, have been used in a number of cases to measure the thermal diffusivity or the thermal conductivity.[8,9] Ideally one would like to use a high-resolution technique which allows for the simultaneous measurement of both static and dynamic thermal quantities. Although some other possibilities exist,[3,10] the fact that in a photoacoustic experiment the signal depends in general on the heat capacity C and the thermal conductivity κ of the sample,[11] allows for rapid simultaneous determination of these quantities even for very small liquid crystal samples.

We have carried out a photoacoustic investigation of several liquid crystal compounds using a completely automatic, PC controlled photoacoustic setup with microphone detection.[12] In this paper we present new data, obtained with a somewhat modified setup, for heptylcyanobiphenyl (7CB), which show some characteristic features encountered for other compounds investigated.

2. METHOD AND EXPERIMENTAL

The photoacoustic effects is based on the periodic heating of the sample induced by the absorption of modulated or chopped (electromagnetic) radiation. In the gas microphone detection configuration the sample is contained in a gas-tight cell. The thermal wave produced in the sample by the absorbed radiation couples back to the gas above the sample and periodically changes the temperature of a thin gas layer above the sample surface. This will result in a periodic pressure change which can be detected by a microphone. The theory for the photoacoustic effect has been developed by Rosencwaig and Gersho.[11] For the photoacoustic microphone signal $Q = qe^{-i\psi}$, with amplitude q and phase ψ (with respect to the radiation modulation) the following equation holds:

$$Q = \frac{\eta\beta I_o \gamma_g P_o}{2\sqrt{2}T_o\kappa l_g a_g(\beta^2 - \sigma^2)} \cdot \left[\frac{(r-1)(b+1)e^{\sigma l} - (r+1)(b-1)e^{-\sigma l} + 2(b-r)e^{-\beta l}}{(g+1)(b+1)e^{\sigma l} - (g-1)(b-1)e^{-\sigma l}}\right] \quad (2.1)$$

In this equation I_o, P_o, T_o, γ_g, are respectively the radiation power density, the cell ambient pressure and temperature and the ratio of the specific heats at constant pressure and volume of the gas. β is the (optical) absorption coefficient of the sample, l is the sample thickness, l_g is the thickness of the gas column above the sample in the cell and $\sigma = (1 + i)a$, with $a = 1/\mu$ the thermal diffusion coefficient. μ is the thermal diffusion length. $\eta = 1 - R$ is the photothermal conversion efficiency, with R the reflectivity. One further has: $b = \kappa_b a_b \mu/\kappa$, $g = \kappa_g a_g \mu/\kappa$, $r = (1 - i)\beta\mu/2$. Here, and also in Equation (2.1), quantities without subscript refer to the sample and the subscripts g and b refer to the cell gas and the sample backing material. When the sample is optically and thermally thick ($e^{\sigma l}$

$>> e^{-\sigma l}, e^{-\beta l}$), it was shown[13] that in Equation (2.1) the contribution of the backing material disappears and one has the following simplified results:

$$q = \frac{\eta\gamma_g P_o I_o t(2t^2 + 2t + 1)^{-1/2}}{2\sqrt{2}\, T_o\, l_g\, (1 + s)\kappa_g a_g^2} \tag{2.2}$$

$$tg\ \psi = 1 + 1/t \tag{2.3}$$

In Equations (2.2) and (2.3) one has $t = \mu\beta/2$ and $s = a\kappa(\kappa_g\, a_g)^{-1}$.

A schematic diagram of our experimental setup is given in Figure 1. The actual photoacoustic measuring cell is given in Figure 2. The sample and the reference material (carbon) are contained is disklike slots (with a diameter of 8 mm and a depth of 0.3 mm) in the same removable gold plated copper sample holder. A He-Ne laser operating at a wavelength $\lambda = 3.39$ μm was chosen because it coincides with the strong absorption band of the C-H groups of the liquid crystal compounds. For the generation of a photoacoustic signal from the reference material we used the visible radiation ($\lambda = 0.64$ μm) of a different He-Ne laser. The switching from the sample to reference, or from one laser beam configuration to the other, can be done automatically and is under the control of a personal computer. In our previous setup[12] the calibration with the reference material had to be carried out by opening the sample cell and replacing the sample with the reference. The new

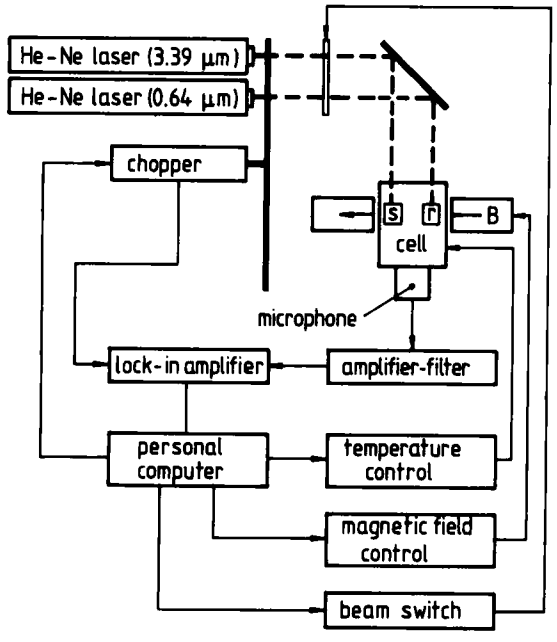

FIGURE 1 Schematic diagram of the photoacoustic setup. *s* refers to the liquid crystal sample and *r* to the reference material (carbon). The arrow indicated by *B* gives the direction of the magnetic field.

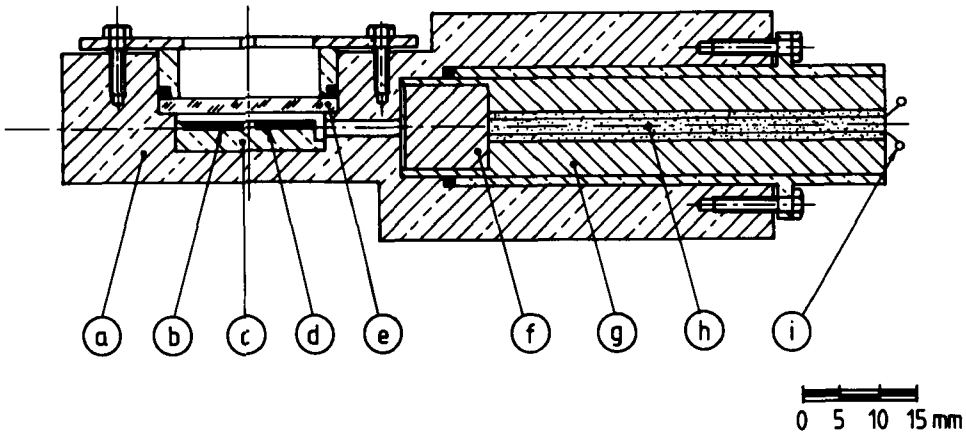

FIGURE 2 Photoacoustic measuring cell with microphone detection a: brass cell body, b: sample, c: sample holder (gold plated copper), d: reference material (carbon), e: quartz window, f: electret microphone, g: microphone holder, h: epoxy, i: microphone leads.

procedure implemented in our present setup greatly enhances the reliability and repeatability of the calibration procedure.

Temperature sensors and electric heaters have been incorporated in the brass body of the photoacoustic measuring cell of Figure 2. The temperature is measured and controlled via digital multimeters and programmable power sources properly interfaced with the PC. An algorithm adjusts every five seconds the heating power in a proportional integrated manner. Stabilisation at fixed temperatures as well as scanning rates as low as a few mK/min can be programmed. At the moment a magnetic field, B, with a maximum value of about 0.5 T, produced by a small electromagnet, can be applied in a direction parallel to the surface of the sample. This field is also controlled via the PC. The two laser beams are modulated mechanically with a chopper. Modulation frequencies between a few hertz and 5 kHz can be set via the computer program. The amplitude and the phase of the PA signals are measured with a dual phase lock-in amplifier in connection with the PC where they are collected and stored for further analysis. At each measuring point five data values for the sample and one for the reference material are usually collected.

3. RESULTS AND DISCUSSION

In this paper we present the results of a series of PA measurements in the isotropic as well as in the nematic phase of heptylcyanobiphenyl (7CB). In an effort to obtain information on the anisotropy of the thermal conductivity, measurements were also carried out in the presence of a magnetic field parallel to the sample surface. In Figure 3 experimental results of the amplitude q and of the phase ψ are given as a function of temperature for $B = 0$ and $B \neq 0$. These results have been

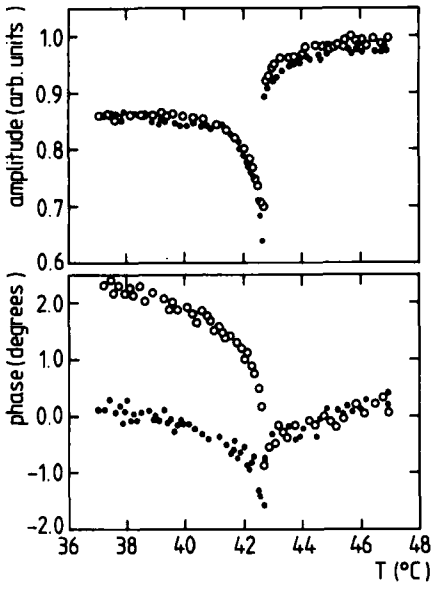

FIGURE 3 Temperature dependence of the amplitude and phase of the photoacoustic signal for the liquid crystal 7CB with a magnetic field of 0.5 T parallel to the sample surface (solid symbols) and without magnetic field (open symbols).

obtained for a modulation frequency of 80 Hz and for a sample thickness of about 0.3 mm. For this thickness, modulation frequency, and the laser wave length λ = 3.39 μm, the PA conditions for thermal and optical thickness were still largely satisfied.

Both the direct amplitude and phase results have been corrected for the temperature dependence on the cell characteristics on the basis of the calibration measurements with carbon as a reference material. This is necessary because the sensitivity of the electret microphone, incorporated in the cell body, to reduce the gas volume and ensure high sensitivity, is temperature (and frequency) dependent. The normalization for the T-dependence of the system sensitivity f_{sys} and the system phase shift ψ_{sys} can be obtained from q_{ref} and ψ_{ref} for the reference material carbon, which can be considered as temperature independent for the temperature ranges involved. The following relations are then applicable:

$$q^m_{ref}(T) = f_{sys}(T) \cdot q_{ref} \tag{3.1}$$

$$\psi^m_{ref}(T) = \psi_{sys}(T) + \psi_{ref} \tag{3.2}$$

$$q^m_s(T) = f_{sys}(T) \cdot q_s(T) \tag{3.3}$$

$$\psi^m_s(T) = \psi_{sys}(T) + \psi_s(T) \tag{3.4}$$

The superscript m refers to the direct experimental signal values. The index s explicitly refers to the sample. Combining the above equations, we obtain the

correct (not influenced by the temperature dependence of the measuring system) photoacoustic signal parameters for the sample:

$$q_s(T) = q_{\text{ref}} \cdot q_s^m(T)/q_{\text{ref}}^m(T) \tag{3.5}$$

$$\psi_s(T) = \psi_{\text{ref}} + \psi_s^m(T) - \psi_{\text{ref}}^m(T) \tag{3.6}$$

In Equations (3.5) and (3.6) one still needs values for q_{ref} and ψ_{ref}. In principle these should be obtainable from the material properties of the reference material and different parameters (e.g. the laser light intensity I_o) of the experiment. It is, however, much easier to use a reference point for the sample, e.g. in the isotropic phase, and calculate q_{ref} and ψ_{ref} which are assumed to be temperature independent, at that temperature from the known (or assumed) sample properties. In this case the absolute accuracy of the derived quantities depend on the accuracy of the sample quantities at the chosen reference point. The temperature dependence of the measured sample quantities is, however, not affected by it. For the data displayed in Figure 3 the highest temperature in the isotropic phase was chosen as reference point.

In both quantities, q and ψ, of Figure 3 the isotropic to nematic phase transition, at about 42.7°C, is clearly visible. The results have been obtained without a special treatment of the sample holder. In the absence of a magnetic field one should normally expect a polycrystalline type distribution of orientationally ordered blocks for the sample in the nematic phase. In the presence of sufficiently large magnetic fields one can arrive at homogeneously oriented samples. Because of the anisotropy in the thermal conductivity[8] it makes a difference for oriented samples whether the thermal wave propagates parallel or perpendicular to the orientation of the long molecular axes. With the $B \neq 0$ configuration chosen here, $\kappa_\perp$ should be applicable. For $B = 0$ and a randomly distributed polycrystalline type orientational order, one could expect an average thermal conductivity $\bar{\kappa} = (\kappa_{//} + 2\kappa_\perp)/3$ for uniaxial mesophases.[14,15] In the isotropic phase one does not expect an effect by the magnetic field for the applied field strengths (with a maximum value of about 0.5 T). This is indeed observed in the experimental results for the isotropic phase in Figure 3, where there are no amplitude or phase differences between $B = 0$ and $B \neq 0$. In the nematic phase there is, however, a clearly visible field effect on the phase of the signal. The amplitude is not affected because it is, for the PA conditions in this experiment, only slightly dependent on the thermal conductivity.

The temperature dependence of C_p and κ can be deduced from the amplitude and the phase results via Equations (2.2) and (2.3), provided one knows also the optical absorption coefficient β, the temperature dependence of the density ρ and of the reflectivity R of the sample. In this case we used a constant value $\beta = 1.6 \times 10^5\ \text{m}^{-1}$. Preliminary measurements of β as a function of temperature did show only a weak temperature dependence. For the temperature ranges considered here the change of R and ρ with temperature is small and can be neglected. In Figure 4 results for the heat capacity C_p and for the thermal conductivity κ, deduced from PA data at four different modulation frequencies, are given. The open symbols are results without a magnetic field. The solid symbols are results with a magnetic

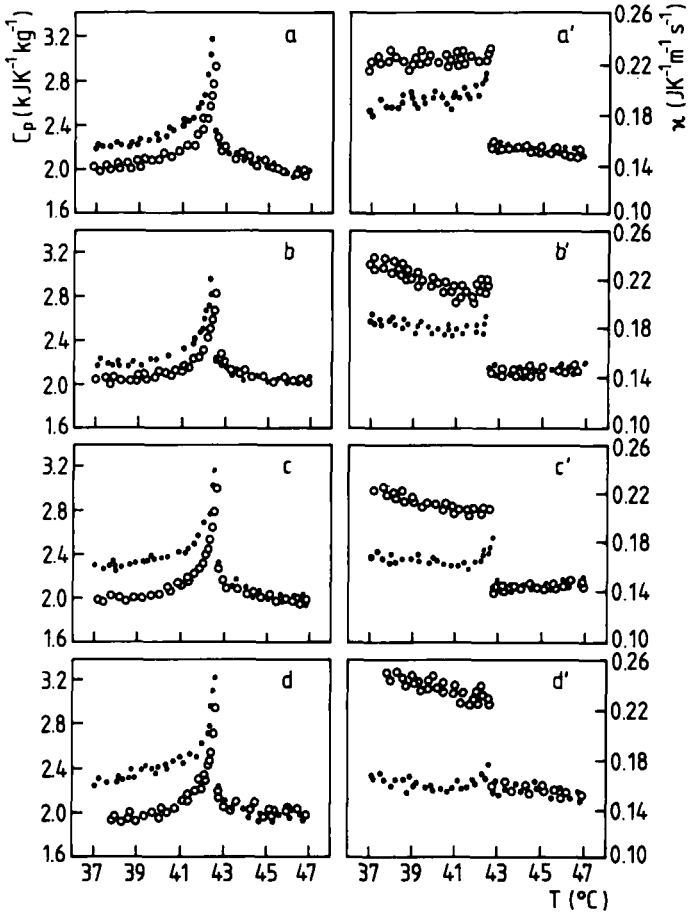

FIGURE 4 Temperature dependence of the heat capacity C_p and the thermal conductivity κ of 7CB as derived from photoacoustic measurements at different modulation frequencies; a, a': 160 Hz, b, b': 120 Hz; c, c': 80 Hz; d, d': 40 Hz. The open symbols represent results without a magnetic field, the solid symbols give results in the presence of a magnetic field of 0.5 T parallel to the sample surface.

field of about 0.5 T parallel to the sample surface. The results for $B = 0$ are essentially the same for the four modulation frequencies. One also notes a substantial increase of the thermal conductivity in going from the isotropic phase to the nematic phase. The difference is much larger here than typically observed between $\bar{\kappa}$ and κ_{is} in the bulk of large size samples,[8] and points in the direction of $\kappa_{//}$ for the N phase, suggesting a surface induced perpendicular alignment of the long molecular axes at the liquid–gas (and the liquid–solid) interface. For the magnetic field parallel to the sample surface, we observe for the N phase an increasing difference between κ ($B = 0$) and κ ($B \neq 0$) with decreasing modulation frequency (or increasing thermal wave lengths μ, from about 12 to 24 μm). For the given field configuration, one would expect a parallel alignment of the molecules and $\kappa_{\perp}$ values for completely oriented samples. For small μ values B is apparently

not large enough to impose a complete parallel alignment of the molecules and arrive at the true $\kappa_\perp$ values. That the parallel alignment is better realized away from the surface, can be concluded from the smaller κ ($B \neq 0$) values obtained for larger μ-values (lower modulation frequencies). For the heat capacity one does not expect a field effect and the differences observed between C_p ($B = 0$) and C_p ($B \neq 0$) are a consequence of the analysis assuming an homogeneously aligned sample, which is, as pointed out above, apparently not the case. To arrive at completely homogeneous parallel samples one would need much larger magnetic fields. It would thus be much easier to arrive at completely homogeneously oriented samples in a field direction perpendicular to the surface of the sample. Modifications of our apparatus to realize this configuration, which is much more difficult to implement, are in progress. Our results, however, show that PA measurements not only offer great possibilities for the investigation of the anisotropy of thermal quantities of liquid crystals but also for the study of surface effects.

References

1. J. Thoen, H. Marijnissen and W. Van Dael, *Phys. Rev. A*, **5**, 2886 (1982).
2. C. W. Garland, *Thermochimica Acta*, **88**, 127 (1985).
3. C. C. Huang, J. M. Viner and J. C. Novak, *Rev. Sci. Instrum.*, **56**, 1390 (1985).
4. J. Thoen, *Phys. Rev. A*, **37**, 1754 (1988).
5. V. S. V. Rajan and J. J. C. Picot, *Mol. Cryst. Liq. Cryst.*, **20**, 55 (1973).
6. R. Vilanove, E. Guyon, C. Mitescu and P. Pieranski, *J. Phys.* (Paris), **35**, 153 (1974).
7. T. Akahane, M. Kondoh, K. Hashimoto and M. Nagakawa, Japan, *J. Appl. Phys.*, **26**, L1000 (1987).
8. W. Urbach, H. Hervet and F. Rondelez, *Mol. Cryst. Liq. Cryst.*, **46**, 209 (1978).
9. M. B. Salamon, P. R. Garnier, B. Golding and E. Buehler, *J. Phys. Chem. Solids*, **35**, 851 (1974).
10. G. Koren, *Phys. Rev.*, **13**, 1177 (1976).
11. A. Rosencwaig and A. Gersho, *J. Appl. Phys.*, **47**, 64 (1976).
12. C. Glorieux, E. Schoubs and J. Thoen, *Mat. Sc. and Eng.* (1989), to appear.
13. M. Marinelli, U. Zammit, F. Scudieri, S. Martellucci, J. Quartieri, F. Bloisi and L. Vicari, *Nuovo Cimento D*, **9**, 557 (1987).
14. P. G. de Gennes, *The Physics of Liquid Crystals*, (Clarendon Press, Oxford, 1974).
15. G. Vertogen and W. H. de Jeu, *Thermotropic Liquid Crystals, Fundamentals*, (Springer-Verlag, Berlin, 1988).